Nanoscale Charge-order Dynamics in Stripe-phase Nickelates Probed via Ultrafast THz Spectroscopy

G. Coslovich*[a], S. Behl[a], B. Huber[a], H. A. Bechtel[b], T. Sasagawa[c], M. C. Martin[b], and R. A. Kaindl[a]

[a]Materials Sciences Division, Lawrence Berkeley National Laboratory, Berkeley, CA USA 94720; [b]Advanced Light Source, Lawrence Berkeley National Laboratory, Berkeley, CA USA 94720; [c]Materials and Structures Laboratory, Tokyo Institute of Technology, Kanagawa Japan 226-8503

ABSTRACT

We discuss equilibrium and ultrafast optical pump-THz probe spectroscopy of the model stripe-ordered system $La_{1.75}Sr_{0.25}NiO_4$. We present a multi-oscillator analysis of the phonon bending mode splitting observed at low temperatures in equilibrium, along with a variational model for the transient THz reflectivity variations. The low temperature splitting is directly related to the formation of the long-range stripe-order, while the background conductivity is reminiscent of the opening of the mid-IR pseudogap. Ultrafast experiments in the multi-THz spectral range show strong THz reflectivity variations around the phonon bending mode frequency (≈11 THz).

Keywords: ultrafast dynamics, nickelate, THz spectroscopy, pseudogap, phonon dynamics, charge order, stripes

1. INTRODUCTION

The dynamics of low-energy excitations and charge transport at the nanoscale is of critical importance for a wealth of fundamental physics and applications, ranging from quasi 1D conduction in nanostructured materials to charge ordering in complex compounds. Recently the important role of charge ordering in cuprate high-temperature superconductors received great attention. Nanoscale charge-order has been linked to the Fermi-arc instability and to the pseudogap phase[1,2], which is ultimately competitive to superconductivity[3-5]. Nonetheless the effects of such nanoscale charge modulations on the transport properties and on the lattice modes of correlated systems have yet to be clarified.

The complex layered material $La_{1.75}Sr_{0.25}NiO_4$ (LSNO) represents an ideal model system to investigate such physics, since at low temperatures electrons organize in quasi 1D atomic-scale rivers of charge, called stripes[6]. Nickelates present the advantage of having chemical and structural similarity to cuprates yet allowing access to real-space carrier correlations without superconductivity at relevant doping levels. This allows isolating the physics of stripes and their dynamics. Recently, ultrafast studies have been very successful in highlighting the relevant cause-effect relations between real-space charge organization and the low-energy excitations[7-9]. However the ability to detect both short and long-range order via a single probe has remained challenging.

Here we report ultrafast optical-pump THz-probe spectroscopy of the stripe-ordered system LSNO. Ultrafast experiments in the multi-THz spectral range show strong THz reflectivity variations around the phonon bending mode frequency (≈11 THz). At low temperatures, this phonon mode exhibits a splitting directly related to the formation of the stripe order, while the background conductivity is reminiscent of the opening of the mid-IR pseudogap[9]. The transient THz probe therefore captures both the electronic and structural dynamics within the same spectrum. The results reveal the dynamical interplay between charge localization and the bending mode folding, providing insight into the symmetry breaking dynamics of nanoscale charge-order.

The manuscript is organized as follows. In Section 2 we review the experimental methods, while Section 3 describes the equilibrium data and the analysis via a multi-oscillator model. Section 4 discusses results from our transient THz reflectivity study.

*email: GCoslovich@lbl.gov; Phone 1-510-486-5264; Fax 1-510-486-6695; www.lbl.gov/kaindl

Ultrafast Phenomena and Nanophotonics XIX, edited by Markus Betz, Abdulhakem Y. Elezzabi, Kong-Thon Tsen, Proc. of SPIE Vol. 9361, 93611F · © 2015 SPIE
CCC code: 0277-786X/15/$18 · doi: 10.1117/12.2080724

2. EXPERIMENTAL SETUP

In this work we perform equilibrium broadband and time-resolved THz reflectivity measurements of $La_{1.75}Sr_{0.25}NiO_4$. The crystals are grown via the floating-zone method and oriented via Laue diffraction. Crystals are then cut along their [1 0 0] surface, and subsequently polished for optimal optical flatness. Per orthorhombic notation, the [1 0 0] surface vector is oriented 45° with respect to the Ni−O bond direction along the *ab*−plane, in which the charge and spin stripes are organized. In this way, both the *ab*-plane and *c*-axis polarized response is optically accessible. At the doping level studied here, long-range stripe patterns of doped holes form below the charge-order transition temperature $T_{CO} \approx 105$ K.

The equilibrium reflectivity $R(\omega)$ is measured with a vacuum FTIR spectrometer (Bruker 66v/S) at the Advanced Light Source (BL 1.4.2). The sample is cryogenically cooled in a liquid helium optical cryostat equipped with mylar and KBr windows. The measurement geometry employed an 11° angle of incidence to obtain the optical properties close to normal incidence. With this geometry the reflectivity is measured in a large spectral range, spanning 10 meV to 1 eV, using a set of different beamsplitters and detectors, for different temperatures and polarizations. Outside this range, the data are smoothly continued from known optical data of nickelates at similar dopings[10,11] and by model functions that approximate the extreme low- and high-frequency limits. Reflectivity data are converted into the conductivity via the Kramers-Kronig constrained variational analysis[12].

Ultrafast pump-probe studies are performed in reflection geometry with the setup outlined in Fig. 1(a). The laser source is a 800 nm, 50-fs Ti:Sapphire regenerative amplifier. A portion of the fundamental laser light is used to pump the sample. We generate and detect THz radiation using thick GaSe crystals, allowing access to the multi-THz range with high spectral resolution. The THz pulse spectrum is optimized to be resonant with the in-plane phonon bending mode of LSNO, i.e., with maximum intensity between 10 and 12 THz.

A schematic representation of the pump-probe experiment is shown in Fig.1(b). The pump pulse excites the LSNO sample, which is kept in the stripe-phase (below T_{CO}), while the THz probe pulse detects both the charge and phonon dynamics. The pump pulse is focused down to a ≈200 μm FWHM spot onto the sample. Based on the available optical data, the penetration depth of the pump beam is ≈125 nm. The penetration depth for the THz probe is generally larger, but varies dramatically across the bending mode resonance. To take into account the strongly frequency dependent penetration depth mismatch we perform a transfer matrix analysis to analyze the time-resolved data, similarly to previous works[9,13].

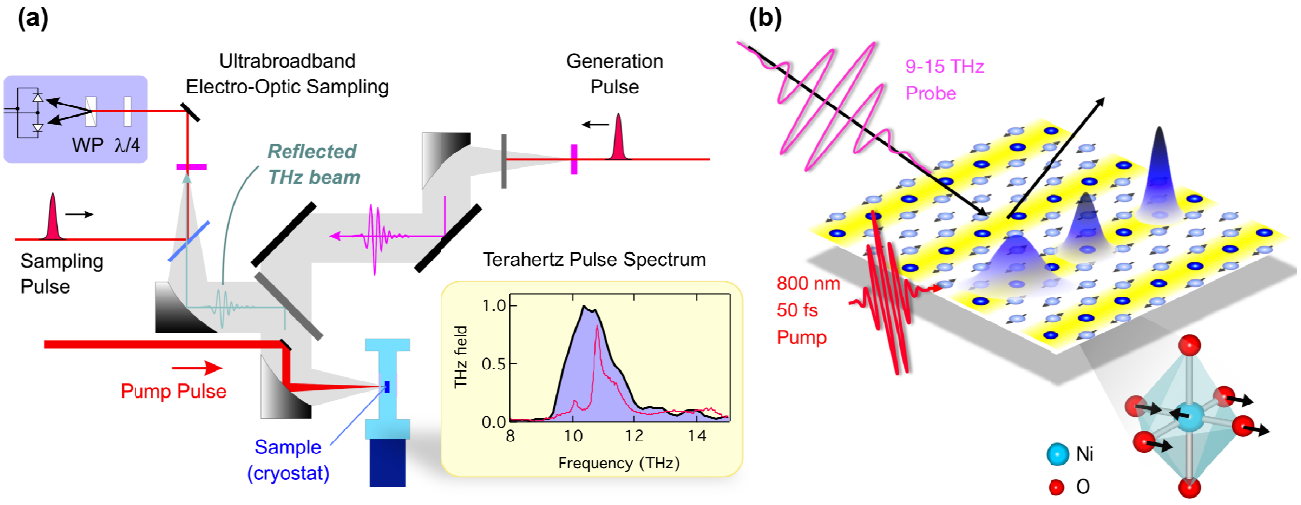

Figure 1. (a) Scheme of the experimental setup used for broadband time-resolved reflectivity studies of LSNO. The inset shows the THz spectrum used in the experiment, along with a typical conductivity profile of the phonon bending resonance. (b) Schematic representation of the pump-probe experiment in the stripe-phase of the LSNO sample. The multi-THz probe detects both the localization dynamics of short-range charge correlations and the modifications of the Ni-O bending mode due to long-range charge order.

3. EQUILIBRIUM CONDUCTIVITY RESULTS AND ANALYSIS

Figure 2(a) shows the in-plane reflectivity spectra of the bending phonon measured on our LSNO sample. Above the charge-ordering transition temperature the phonon behaves as a single Lorentz oscillator, while below 110 K three sharp resonances appear. These sharp features become stronger as the temperature is lowered well into the stripe-ordered phase, suggesting a clear connection to the establishment of long-range ordering. Such behavior is often observed in materials exhibiting charge order and it can be associated with the phonon zone folding at q_{CO} due to superlattice modulation[14].

To analyze the observed results it is necessary to introduce a multiplet of N Lorentz oscillators centered around the high-temperature bending mode frequency. Thus the complex dielectric function can be expressed as

$$\varepsilon(\omega) = \varepsilon_0 + \sum_{j=1}^{N} \frac{\omega_{p,j}^2}{(\omega^2 - \omega_{0,j}^2) - i\Gamma_j \omega} \tag{1}$$

where ε_0 is the background complex dielectric constant, and $\omega_{p,j}, \omega_{0,j}, \Gamma_j$ are respectively the plasma frequency, the resonance frequency and the linewidth of the j-oscillator. From the complex dielectric function we directly calculate the reflectivity and conductivity to be compared to the experimental data.

Figure 2(b) illustrates the choice of the number N of phonon modes to be used in the model. In the charge ordered state the experimental data between 350 and 380 cm^{-1} are better reproduced when using a total of four phonon modes. These phonons comprise a peak remnant of the broad high-temperature phonon and three additional sharp modes.

The corresponding equilibrium conductivity data around the bending mode, obtained from Kramers-Kronig constrained variational analysis, are shown in Figure 3. The spectrum confirms the appearance of a multiplet of phonon modes below T_{CO}. The fitting curves show a good agreement with the data, in turn yielding the resonance frequencies and oscillator strengths of these modes as a function of temperature (not shown). Our analysis indicate that these three new sharp

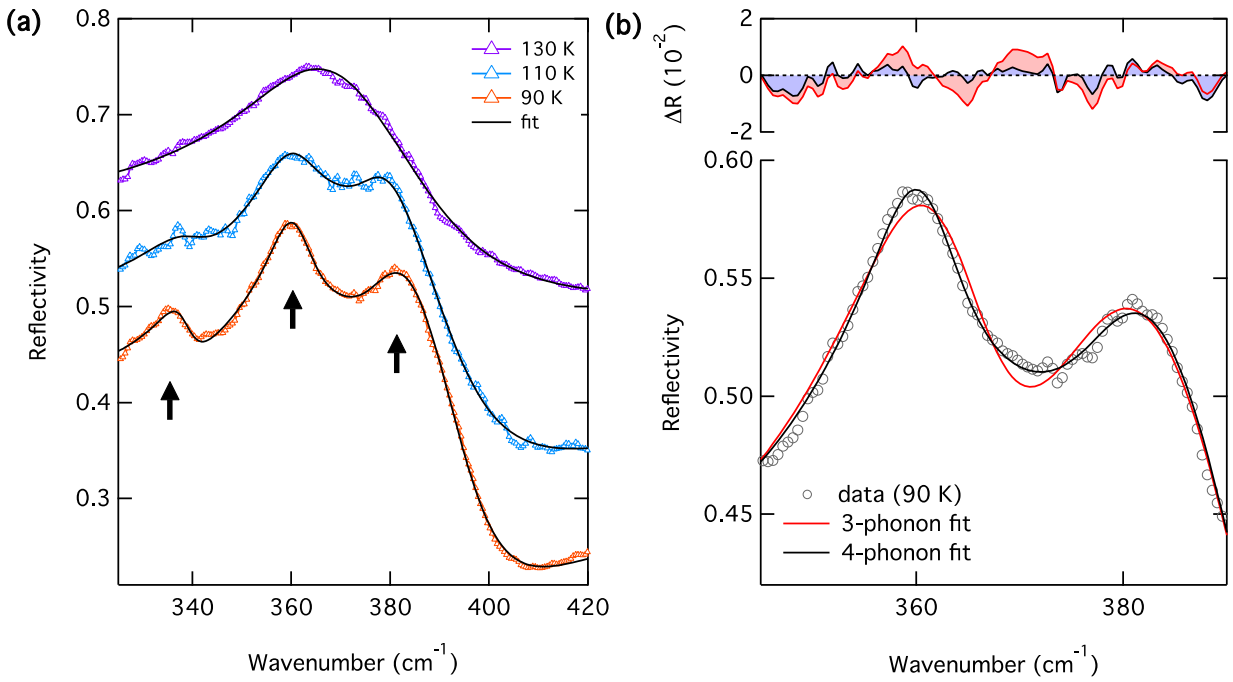

Figure 2. (a) Equilibrium reflectivity of $La_{1.75}Sr_{0.25}NiO_4$ at different temperatures across T_{CO} and corresponding multi-oscillator fits. The arrows indicate the sharp phonon resonances appearing in the charge-ordered state. Curves are offset vertically for clarity. (b) Detail of the multi-oscillator model. The red line represents a tentative fit with $N = 3$ modes, while the black line is the best model, with $N = 4$. The top graph shows the two respective residuals.

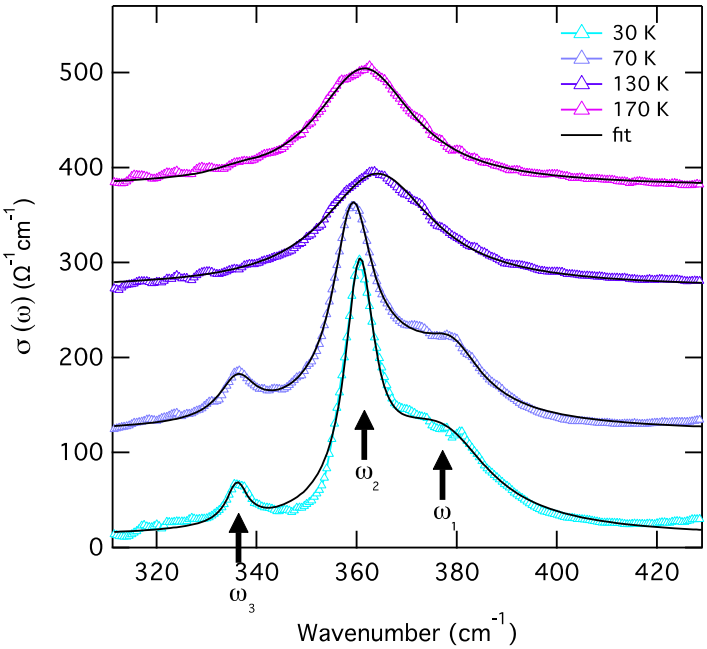

Figure 3. Equilibrium conductivity of $La_{1.75}Sr_{0.25}NiO_4$ at different temperatures and corresponding best fit. Curves are offset vertically for clarity. The arrows indicate the sharp phonon resonances (j = 1,2,3) appearing in the charge-ordered state.

resonances are a direct consequence of long-range ordering, and that their peak intensity can be used to probe the ordered state, as a complementary technique to X-Ray Diffraction (XRD)[8].

We also note that the conductivity background at the bending mode frequency is affected by the presence of the mid-IR pseudogap, which has been described in detail in Ref. [9]. The pseudogap indicates the onset of charge localization and is therefore an indicator of short-range stripe correlations. In conclusion, a probe resonant with the in-plane phonon bending mode in LSNO can detect both short- and long-range charge ordering.

4. ULTRAFAST THZ SPECTROSCOPY RESULTS

To probe the dynamics of the short- and long-range order we perform ultrafast THz spectroscopy resonant on the Ni-O bending mode. We can achieve a resolution $\Delta\nu < 0.2$ THz by scanning up to 8 ps of the pump-probe THz field trace, as shown in Figure 4(a). This resolution is necessary to be able to detect variations of the sharp phonon resonances associated with long-range ordering. The pump fluence is set to ≈ 0.5 mJ/cm^2 and the sample temperature is maintained at 20 K.

The reflected THz electric field around $t_{THz} \approx 0$ ps promptly responds to photo-excitation, while a more complex structure appears in the time-domain THz trace at later pump-probe delay times. The corresponding spectral responses are shown in Figure 4(b). At a pump-probe delay of $\Delta t = 0$ ps, the broad increase of the reflected field indicates the modulation of the electronic background expected for the closing of the pseudogap[9]. At $\Delta t = 0.6$ and 1.8 ps we observe a fast decay of this broad component and the appearance of sharp negative features in proximity to the phonon resonances observed at equilibrium (Section 3).

To interpret the experimental results we consider variations of the multi-oscillator model presented in Section 3. To take into account the inhomogeneity of the probed volume, due to the pump and probe penetration depth mismatch, we perform a transfer matrix calculation. The variational model reproduces well the data, with the pseudogap signal dominating at early pump-probe delays and the sharp phonons being suppressed at later delay times.

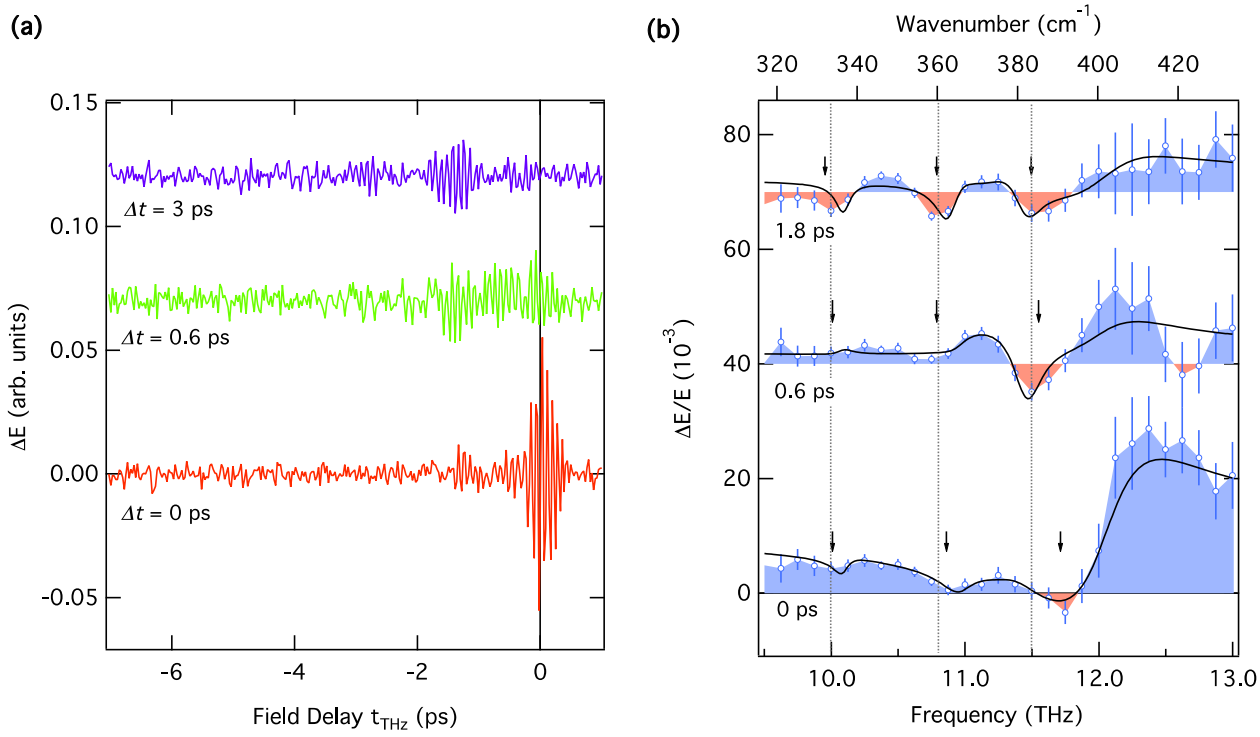

Figure 4. **(a)** THz temporal traces of the transient variations of the reflected electric field at different pump-probe delays (Δt = 0, 0.6, and 3 ps). **(b)** THz pump-probe spectral traces at indicated pump-probe 0, 0.6, and 1.8 ps delay times. Dotted vertical lines mark the positions of the three sharp phonon resonances at equilibrium from Fig. 3(a). The arrows mark the negative dips in the pump-probe data. Solid lines: variational multi-oscillator fits. Curves are offset vertically for clarity.

Our results indicate the suppression of the sharp phonon signal after photo-excitation, where further analysis shows a slower relaxation dynamics ($\tau > 3$ ps). This timescale is compatible with the amplitude dynamics of long-range order obtained from time-resolved X-Ray diffraction experiments[8]. The dynamics of the fast broad spectral component ($\tau < 1$ ps) is in agreement with the localization timescale of short-range stripe correlations in LSNO[9]. The observation of clear signatures of both short-and long-range stripe correlations in the THz spectral response of LSNO provides unprecedented insight into the lattice zone-folding dynamics during the suppression of an electronic superlattice modulation.

5. CONCLUSIONS

To summarize, we discussed equilibrium and ultrafast optical pump-THz probe spectroscopy of the model stripe-ordered system $La_{1.75}Sr_{0.25}NiO_4$. Ultrafast experiments in the multi-THz spectral range show strong THz reflectivity variations around the phonon bending mode frequency (≈11 THz). The signal is interpreted as large modulations of sharp phonon side peaks due to the charge-ordering transition. We discuss the multi-oscillator analysis of the phonon splitting in equilibrium and the variational model used to reproduce the transient THz reflectivity variations. Our ultrafast THz study discussed here constitutes a novel approach to probe the symmetry breaking dynamics of nanoscale charge-order.

ACKNOWLEDGMENTS

We thank W.-S. Lee and Z.-X. Shen for fruitful scientific discussions and their contribution in the early stage of this work. This research was supported by the U.S. Department of Energy, Office of Basic Energy Sciences (DOE BES), Division of Materials Sciences and Engineering under contract DE-AC02-05CH11231 at Lawrence Berkeley National Laboratory (G.C., S.B., B.H., R.A.K.). The Advanced Light Source is supported by DOE BES under the same contract (H.B., M.M.). B.H. and S.B. acknowledge fellowship support from the German Academic Exchange Service (DAAD) and participation in an exchange program with the U.C. Berkeley Nanosciences and Nanoengineering Institute.

REFERENCES

[1] Parker, C. V., Aynajian, P., Neto, E. H. D. S., Pushp, A., Ono, S., Wen, J., Xu, Z., Gu, G., Yazdani, A., "Fluctuating stripes at the onset of the pseudogap in the high-Tc superconductor $Bi_2Sr_2CaCu_2O_{8+x}$," Nature **468**(7324), 677 (2010).

[2] Comin, R., Frano, A., Yee, M. M., Yoshida, Y., Eisaki, H., Schierle, E., Weschke, E., Sutarto, R., He, F., *et al.,* "Charge Order Driven by Fermi-Arc Instability in $Bi_2Sr_{2-x}La_xCuO_{6+\delta}$," Science **343**(6169), 390–392 (2014).

[3] Hashimoto, M., Nowadnick, E. A., He, R.-H., Vishik, I. M., Moritz, B., He, Y., Tanaka, K., Moore, R. G., Lu, D., *et al.*, "Direct spectroscopic evidence for phase competition between the pseudogap and superconductivity in $Bi_2Sr_2CaCu_2O_{8+\delta}$," Nat. Mater., **14**(1), 37–42, (2014).

[4] Kondo, T., Khasanov, R., Takeuchi, T., Schmalian, J., Kaminski, A., "Competition between the pseudogap and superconductivity in the high-Tc copper oxides," Nature **457**(7226), 296–300 (2011).

[5] Coslovich, G., Giannetti, C., Cilento, F., Dal Conte, S., Abebaw, T., Bossini, D., Ferrini, G., Eisaki, H., Greven, M., et al., "Competition Between the Pseudogap and Superconducting States of $Bi_2Sr_2Ca_{0.92}Y_{0.08}Cu_2O_{8+\delta}$ Single Crystals Revealed by Ultrafast Broadband Optical Reflectivity," Phys. Rev. Lett. **110**(10), 107003 (2013).

[6] Tranquada, J., Kivelson, S., Uchida, S.-I., Fink, J., Tajima, S., "Preface," Phys. C **481**, 1–2 (2012) and following articles of the same issue.

[7] Fausti, D., Tobey, R. I., Dean, N., Kaiser, S., Dienst, A., Hoffmann, M. C., Pyon, S., Takayama, T., Takagi, H., et al., "Light-Induced Superconductivity in a Stripe-Ordered Cuprate," Science **331**(6014), 189–191 (2011).

[8] Lee, W. S., Chuang, Y. D., Moore, R. G., Zhu, Y., Patthey, L., Trigo, M., Lu, D. H., Kirchmann, P. S., Krupin, O., et al., "Phase fluctuations and the absence of topological defects in a photo-excited charge-ordered nickelate," Nat. Commun. **3**, 838 (2012).

[9] Coslovich, G., Huber, B., Lee, W. S., Chuang, Y. D., Zhu, Y., Sasagawa, T., Hussain, Z., Bechtel, H. A., Martin, M. C., et al., "Ultrafast charge localization in a stripe-phase nickelate," Nat. Commun. **4**, 2643 (2013).

[10] Ido, T., Magoshi, K., Eisaki, H., Uchida, S., "Optical study of the $La_{2-x}Sr_xNiO_4$ system: Effect of hole doping on the electronic structure of the NiO_2 plane," Phys. Rev. B **44**(21), 12094–12097 (1991).

[11] Jung, J., Kim, D., Noh, T., Kim, H., Ri, H., Levett, S., Lees, M., Paul, D., Balakrishnan, G., "Optical conductivity studies of $La_{3/2}Sr_{1/2}NiO_4$: Lattice effect on charge ordering," Phys. Rev. B **64**(16), 165106 (2001).

[12] Coslovich, G., Huber, B., Lee, W. S., Chuang, Y. D., Zhu, Y., Sasagawa, T., Hussain, Z., Bechtel, H. A., Martin, M. C., et al., "Ultrafast mid-infrared spectroscopy of the charge- and spin-ordered nickelates," Proc. SPIE, 8623, 862308 (2013).

[13] Kaiser, S., Hunt, C. R., Nicoletti, D., Hu, W., Gierz, I., Liu, H. Y., Le Tacon, M., Loew, T., Haug, D., et al., "Optically induced coherent transport far above Tc in underdoped $YBa_2Cu_3O_{6+\delta}$," Phys. Rev. B **89**(18), 184516 (2014).

[14] Homes, C., Tranquada, J., Buttrey, D., "Stripe order and vibrational properties of $La_2NiO_{4+\delta}$ for δ=2⁄15: Measurements and ab initio calculations," Phys. Rev. B, **75**(4), (2007).